Study on the Behaviours of Lightweight Sintagg Sintered Fly Ash Aggregates Geopolymer Concrete (Sustainable Material) Beams Using MIF

Pushpendra Singh Palash[1] and Priyanka Dhurvey[2]

[1]Ph.D. Research Scholar, Department of Civil Engineering, MANIT-Bhopal-462003 (Madhya Pradesh), India.

[2]Assistant Professor, Department of Civil Engineering, MANIT-Bhopal-462003 (Madhya Pradesh), India.

Abstract

Challenges arising because of the scarcity of coarse aggregates in construction and the environmental impact of mining, natural coarse aggregates from mountains have led to an urgent need for sustainable alternatives. Traditionally, Sintagg sintered fly ash lightweight aggregate (SSFAA) has been identified as a promising substitute for coarse aggregates. It is derived from fly ash generated during the production of thermal power plants. In the production process, a solution of sodium silicates (water glass) and a 12.5 M sodium hydroxide solution are used as the alkaline activator liquids. The ratio of sodium hydroxide to sodium silicates is maintained at 2.0 for optimal results. A modified geopolymer concrete has been made by using sintered fly ash aggregate. Sintered fly ash aggregate density is approx. half of the normal aggregate. So, the geopolymer concrete made by using sintered fly ash aggregate is lightweight. A modified geopolymer concrete using different sizes of aggregate has been prepared. An accurate assessment of stress and displacement throughout the depth of the beam by MIF based on the elastic properties of lightweight geopolymer concrete material is obtained, without conducting any experimental program while bending theory is based on formulas. MIF results are almost the same as the bending theory thus showing that MIF can be applied to the analysis of lightweight beams. Consequently, it may be concluded that MIF is supported by the validation of its results with bending theory.

Keywords: - Lightweight Geopolymer concrete, Sintered Fly ash Aggregate, Method of initial functions Beams (MIF).

1. Introduction

A major issue observed during earthquakes is the loss of life caused by structural collapses under the heavy load of conventional concrete structures. This issue arises from the high mass density of traditional geopolymer concrete compared to lightweight geopolymer

concrete. The utilization of Ground Granulated Blast Furnace Slag (GGBS) and fly ash in lightweight geopolymer concrete represents a sustainable construction approach that addresses this problem.

This method involves incorporating waste materials from coal combustion, particularly from thermal power plants like those in Sarni, India. Additionally, the inclusion of sintered fly ash aggregate, known as Sintagg, further enhances the properties of geopolymer concrete, making it an environmentally friendly and efficient construction solution. Sintagg sintered fly ash lightweight aggregate is produced by heating coal combustion ash at high temperatures and is then utilized in geopolymer concrete to create lightweight structures.

Typically ranging from 4mm to 12mm in size, Sintagg sintered fly ash lightweight aggregate contributes significantly to the lightweight properties of geopolymer concrete. The mass density of conventional geopolymer concrete ranges from 2200 to 2600 kg/m³, whereas the mass density of lightweight geopolymer concrete is considerably lower, ranging from 300 to 1900 kg/m³. Lightweight geopolymer concrete (LWC) reduces the dead load of structures, improves thermal and acoustic insulation properties, and lowers the cost of haulage and handling.

LWC can be used for various engineering applications, such as building construction, bridge deck pavements, and architectural elements. Depending on the usage, LWC is classified as structural lightweight concrete, non-load-bearing concrete, or insulating concrete. Notably, LWC exhibits higher specific strength compared to conventional concrete, making it a promising material for earthquake-resistant construction.

The most common types of LWC are:

- Light-Weight Aggregates Concrete (LWAC) – The conventional aggregates are replaced using lightweight aggregates (fine or coarse aggregates) to lower the mass density of concrete.
- Aerated concrete / Foam concrete – The introduction of an air bubble or foam generating compounds to the fresh concrete increases its volume, hence reducing the mass density of concrete.
- No-fines concrete – The name itself suggests, the fines are not present in the concrete.

In this research, we have completely replaced the coarse aggregates with sintagg fly ash aggregates.

Modern construction methods have increased the demand for lightweight concrete in various structural applications [1]**.** Production of structurally high-strength lightweight concrete is also now possible because of the advancement in the field of cement and concrete

technology [2, 3]. The aggregates are frequently made from industrial waste products as fly ash [4]. Fly ash is very harmful to humans and affects environmental degradation [5]. To fulfill this gap, the feasibility of using sintered lightweight aggregate in concretes has been studied. Significant environmental issues have been brought because of deforestation and the removal of conventional aggregates derived naturally from riverbeds, lakes, and other areas of water. Hence the government imposes restrictions on the excavation of aggregates from natural places like hills and mountains. The problem has been solved by replacing the natural aggregate with sintered fly ash aggregate which is in the size range of 4-8mm and 8-12mm.

2. Method of initial functions (MIF): -

The inception of the idea for MIF dates to 1951 when Malieev first proposed it, with further development by Vlasov in 1955. The concept involves utilizing beams constructed from various sizes of aggregate to achieve optimal packing density. This model is based on understanding the properties of beams without constructing them. Evaluating laminated beams poses a challenge due to their unique composition. In MIF, the equations governing the flexure of these beams are derived without relying on assumptions about their physical behavior, employing the method of initial functions (MIF) [6,7,8,9]. This analytical approach, rooted in elasticity theory, yields precise results for diverse problems, irrespective of the stress-strain state of the structural element. In recent times, MIF has found widespread application in analyzing various issues. Notably, it enables the solution of three-dimensional elasticity equations for spherical cylindrical shells by employing Taylor series expansions to compute stresses and displacements [18].

Notations [18, 31]

L	Beam length
H	Beam depth
b	Beam width
d	Density of lightweight geopolymer concrete
E	Young’s modulus of elasticity of lightweight geopolymer concrete
F	Compressive strength of lightweight geopolymer concrete
G	Shear modulus of elasticity of lightweight geopolymer concrete

μ	Poisson's ratio
v	vertical displacement
rx	bending stress

3. Literature review:

3.1 Development of Geopolymer Composites:

Geopolymerization occurs in three stages: (a) dissolution; (b) transportation or orientation; and (c) polycondensation. The percentages of calcium hydroxide and calcium silicate, molarity, Si/Al ratio, and the binder properties are all parameter that affect the strength of GPC **[10].** Lightweight geopolymer concrete has Fly ash and GGBS as binders, alkaline solution as an activator, and fine and coarse aggregate used to prepare mix composite. The most common Alkaline Solution is a combination of alkali hydroxide (Sodium hydroxide) and alkali silicate (Sodium silicate). Describes the three stages of geopolymerisation as (a) deconstruction or destruction (dissolution in alkaline solution), (b) polymerization of alumina/silica–hydroxyl species, and (c) stabilization, small gels formed are probably transformed into large networks through reorganization. The reactions of geopolymerisation take place through a series of exothermic processes **[12,13]**.

3.2 Literature on MIF:

Method of Initial Functions is used for the analysis of beams under symmetric central loading and uniform loading **[14].** For the analysis of the free vibration of rectangular beams with any depth, the MIF is used. The frequency values are calculated using the Timoshenko beam theory and present the analysis for different values of Poisson's ratio **[15].** MIF is used to create the governing equations for composite laminated deep beams. The proposed beam theory can be used for a wide range of beam depths **[16].** The analysis of modified deep beams is conducted using the method of initial function, and the outcomes are compared with the existing theory **[17,31].**

4. Material and Methods

4.1 Aggregates

Sintered fly ash lightweight aggregates (SFA), produced by sintering fly ash (IS Code 9142 Part 2), are utilized as coarse aggregate. Sintered aggregates are artificially produced round-

shaped aggregates with hard interior honeycombed spongy structures by thermal processing. It is manufactured by Litagg Industries Private Limited Ahmadabad, INDIA.

Table 1: Physical Properties of Aggregate

Properties	Value
Aggregate size	4-8mm; 8-12mm
Aggregate strength	More than 40MPa
Bulk density	@ 850Kg/M^3
Bulk porosity	35-40%
Water absorption	17%
Aggregate shape	Rounded pallets

Table 2: Physical properties of a different mix of SFA

S. No.	Mix		Sample	% Combination	Specific Gravity	Water Absorption
1	Unitary		A_1	(4-8mm=100%) & (8-12mm=0%)	1.771	19.46
2			A_5	(4-8mm=0%) & (8-12mm=100%)	1.779	19.07
3	Binary		A_2	(4-8mm=75%) & (8-12mm=25%)	1.796	19.50
4			A_3	(4-8mm=50%) & (8-12mm=50%)	1.772	18.57
5			A_4	(4-8mm=25%) & (8-12mm=75%)	1.775	21.59

Cubical samples of size 150 X 150 X 150 mm were prepared for determining the compressive strength on 3, 7, and 28 days. Sun-dried curing of the specimens was done at ambient temperature. SFA was segregated into five different ranges based on the varying proportion of aggregate size used in preparing samples as shown in Table 2. According to IS 2386-3, each combination's specific gravity and water absorption were calculated **[18].** The gradation of aggregate for A_1, A_2, A_3, A_4, and A_5 are given.

4.2 Fly ash: - If we are using only fly ash in geopolymer concrete then heat curing of 45-90^{o}C is required due to low calcium amount in a binder (fly ash). Low initial setting is due to low calcium content in fly ash so heat curing is needed necessary to gain early strength.

Table 3: Chemical characteristic of fly ash

Properties	Value
SiO_2	55
Al_2O_3	26
Fe2O	7
CaO(Lime)	9
MgO	2
SO_3	1

4.3 GGBS: - GGBS-based Geopolymer concrete due to the good amount of calcium content in GGBS-based Geopolymer concrete gain good initial strength. So, it does not require heat curing for early strength gain. No heat curing is required only ambient curing is required.

Table 4: Chemical characteristic

Properties	Value
SiO_2	33
Al_2O_3	13.46
Fe2O	0.31
CaO(Lime)	41.7
MgO	5.99
SO_3	2.74

5. Mix design of Geopolymer concrete

5.1 Materials properties: -

- **Binder Content: -**GGBS, fly ash materials is used in geopolymer concrete as binder content. Following properties are found before the design mix i.e. density, initial and final setting time.
- **Fly ash: -**To find out the physical properties of SSFA like water absorption, specific gravity, bulk density, and gradation of aggregate.
- **Mixing Composition: -**

Five series mixes were used in this research paper

1. Alkaline liquid to binder ratio is 0.7%
2. Sodium hydroxide to sodium silicate is 2.0.
3. Temperature curing is ambient.

4. Molarity of NaOH is 12.5.
5. GGBS &Fly ash Combination (70:30)

- **Sample preparation: -**

Based on the size of coarse aggregates

- A_1- (4-8mm=100%) & (8-12mm=0%)
- A_2- (4-8mm=75%) & (8-12mm=25%)
- A_3- (4-8mm=50%) & (8-12mm=50%)
- A_4- (4-8mm=25%) & (8-12mm=75%)
- A_5- (4-8mm=0%) & (8-12mm=100%

5.2 Manufacturing process

At this stage, mix design process of GPC mix as per Indian Standard code guidelines was carried out. On finalization of the mix design, the following laboratory tests were undertaken;

- Mix Design for GPC

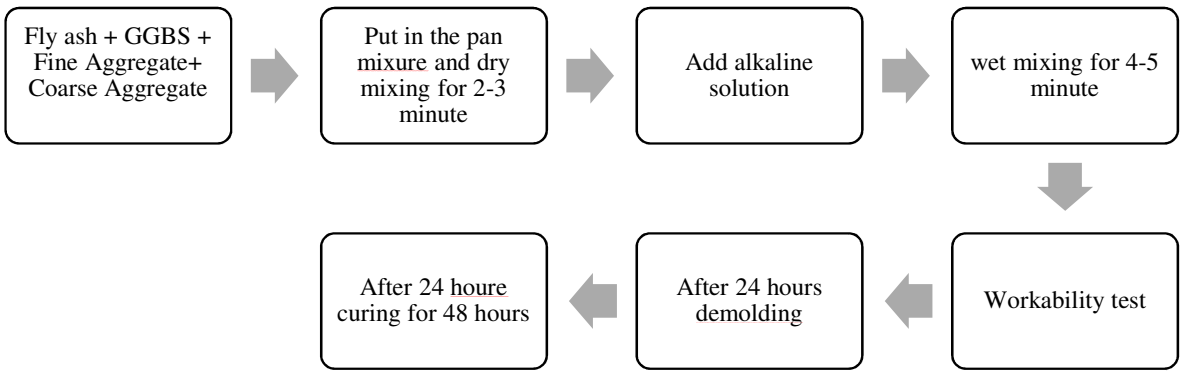

Figure 1: Geopolymer concrete manufacturing process flow chart

- Fresh state properties of GPC mix
- Hardened state properties of GPC mix
- Cube Compression Test

Figure 2: fly ash aggregate

Figure 3: Raw materials fly ash aggregate, sand, GGBS, fly ash

Figure 4: NaOH and Sodium Silicate

Figure 5: Geopolymer concrete fresh state

Figure 6: After Demoulding Sample

Table 5: Configuration of coarse aggregate in concrete mixes

Materials			Quantity in Kg				
		A_0	A_1	A_2	A_3	A_4	A_5
GGBS &Fly ash		567	567	567	567	567	567
Fine aggregate		889	889	889	889	889	889
Coarse aggregate		1207.04	0	0	0	0	0
Coarse aggregate	4-8mm	0	554	416	277	139	0
	8-12mm	0	0	139	277	416	554
Alkaline solution		340	340	340	340	340	340

6. Results and Discussion

6.1 Testing of concrete cubes of Compressive Strength

The compressive strength of the geopolymer concrete cube was assessed following the IS516:1959 standard. Before calculating compressive strength, each cube mold was weighed to determine the density of the geopolymer concrete. Testing of the GPC cube was conducted using a compressive strength testing machine with a capacity of 3000KN. The results obtained for the compressive strength of geopolymer concrete samples A_0, A_1, A_2, A_3, A_4, and A_5 are depicted in Figure 7.A_0 is normal aggregate mix concrete whose compressive strength is high but on the other hand, when we have prepared sintered fly ash aggregate based geopolymer concrete A_2 as specified before, achieves the maximum strength due to appropriate gradation of aggregates. Almost all the mixes have shown the development of strength with age and thus achieved the desired characteristic compressive strength.

Table 6: Strength development of GP with SFA

Mix	Compressive Strength (MPa)				
	3d	**7d**	**14d**	**21d**	**28d**
A_0	46.3	57.44	63.11	69.04	76.74
A_1	26.5	35.9	51.3	55.2	69.6
A_2	28.3	37.9	56	66.37	71.1
A_3	26.4	48	52.3	60.9	69.8
A_4	25.2	47.1	51	57	64.6
A_5	25	43.3	47.6	55.9	60.5

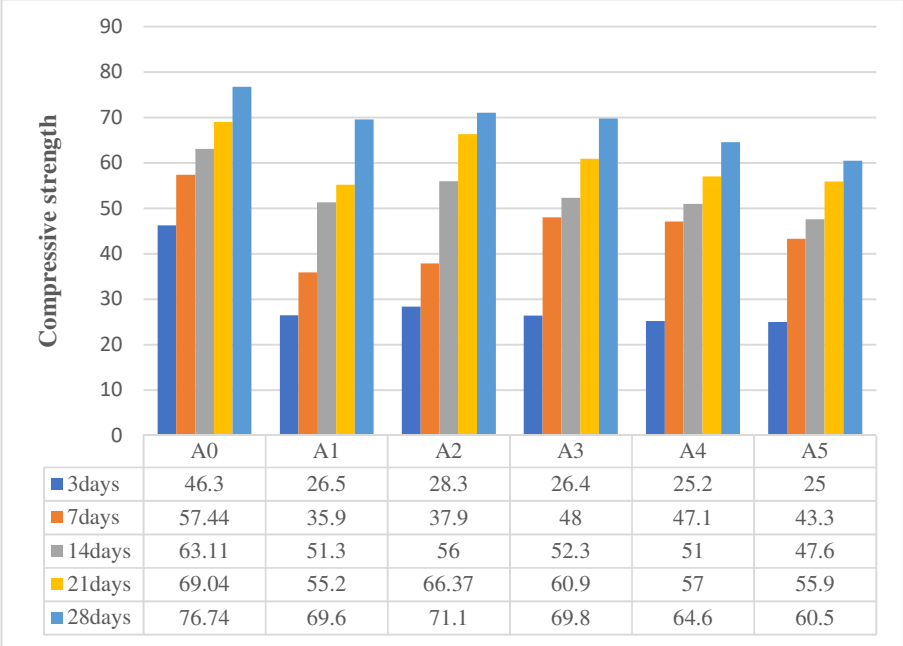

Figure 7: Compressive strength with different combinations of SFA at different curing ages.

6.2. Composite beam analysis using MIF and bending theory: - MIF is used to determine the stresses and displacement of geopolymer concrete beams. Fly ash aggregate is used in place of coarse aggregate to create lightweight geopolymer concrete. By using conventional theories, it is impossible to examine the lightweight geopolymer concrete beam made of such composite materials. Hence, without performing any flexural tests or

experimental analyses, MIF is used in this study to examine the geopolymer concrete beams using their elastic properties and theoretical loads.

The elastic properties (E, G, and μ) of Modified geopolymer concrete were derived from the cube test results. The theoretical load denoted as P0, is determined based on the compressive strength characteristics of the geopolymer concrete cubes after 28 days of curing at ambient temperature, following the principles of limit state design for beams [14].

For analysis, a point load is assumed to be applied to the top surface of the beam. The expression representing this point load in the form of a sine series is provided as follows:

$$P(x) = \frac{P0}{l}_0 + \sum_{n=1}^{\infty} \left(\sin \frac{\pi x}{l}\right) \ldots\ldots\ldots\text{(i)}\textbf{[14]}$$

At every 80 mm depth of the beam, the stresses and displacement are calculated and compared with theoretical results. **[27].**

6.3. Elastic Modulus

In the case of geopolymer concrete subjected to ambient curing, the maximum compressive strength tested is close to 55 MPa, in addition, there is a relatively weak correlation between the elastic modulus and compressive strength. Based on this finding, there is a possibility to conduct a regression analysis on the entire test data set while ignoring the effect of curing. The linear equation shown below, with its greatest R^2 value of 0.642, was confirmed to be correct in this situation.

$$E_c = 4 \text{ X} 10^{-6} \text{X } (\gamma_c)^{2.66} \text{ X } (f_c')^{0.5} \ldots\ldots\ldots\ldots\ldots\ldots\ldots\ldots\ldots\ldots\text{(ii)}\textbf{[15]}$$

Where, E_c and fc' are measured in N/mm^2. The predictions of Posi et al. **[16]** is similar to that of the proposed equation (Equation (ii)) but slightly underestimates test data for GPC of compressive strength greater than about 50 MPa. ACI 318 **[17]** equation overestimates the test data for concrete having compressive strength lower than 50 MPa, while the proposal of Cui et al. **[17]** highly underestimates tested elastic modulus. In general, the equation provided by Jamal **[15]** states that lightweight concrete moderately overestimates the test data. The model given by Nath and Sarkar **[19]** and Hassan et al. **[20]** is moderately accurate but tends to underestimate test data for GPC of compressive strength higher than 40 MPa.

6.4. Poisson's Ratio

There are less test results available for Poisson's ratio compared to the other geopolymer concrete properties. 99 different data samples in total were collected for this study. Also, it appears that there were no equations for the prediction of the Geopolymer concrete Poisson's ratio. When compared to the other mechanical parameters, the Poisson's ratio and compressive strength show a relatively weak correlation with each other. For this reason and in addition to

address this weakness, it is preferable to create a correlation between compressive strength and the normalized Poisson's ratio (υ /fc')**[14].**

In the analysis correlating Poisson's ratio with compressive strength, a significant coefficient of determination is observed. Through regression analysis, the finalized equation for predicting Poisson's ratio is derived as follows:

$$\mu = \frac{0.2324}{(Fc)\text{^}0.093} \text{.....(iii)}$$

The following beam dimension values were selected for the specified problem.

H = 400mm; L = 3000mm and b = 150mm.

The boundary condition of simply supported edges is given by

X = Y = v = 0; at x = 0 and x = 1.

20N/mm^2 of uniformly distributed load is applied to the surface of the beam. And beam is simply supported.

6.5. Analytical findings and discussion

The stresses and displacement that were calculated analytically using the MIF and bending theory are shown in the table below. Without using an experimental analysis, the beams are analyzed using the elastic characteristics and loads. The comparison is done with bending theory and is analyzed for different percentages of coarse aggregate used in lightweight materials in the beams.

Table 7: Load and elastic properties

Mix	Density Kg/m^3	Compressive strength (N/mm^2)	E (N/mm^2)	G (N/mm^2)	μ
A_1	1907.2	69.6	17750.8	0.15663	10265.6
A_2	1907.2	71.1	17941.1	0.15632	10372.8
A_3	1907.2	69.8	17776.3	0.15659	10279.9
A_4	1907.2	64.6	17101.3	0.15772	9899.28
A_5	1907.2	60.5	16549.8	0.15868	9587.97

6.6. Sintered fly ash aggregate mix

Table 8: A_1 mix material deflection and bending theory calculation

Depth (mm)	MIF displacement v (mm)	MIF Stress σ_x (N/mm^2)	Bending Theory displacement v (mm)	Bending Theory Stress σ_x (N/mm^2)
0	18.41	-720.76	18.57	-843.75
80	18.46	-432.46	18.57	-506.25
160	18.51	-144.15	18.57	-168.75
240	18.52	143.87	18.57	168.75
320	18.52	434.35	18.57	506.25
400	18.56	717.20	18.57	843.75

Table 9: A_2 mix material deflection and bending theory calculation

Depth (mm)	MIF displacement v (mm)	MIF Stress σ_x (N/mm^2)	Bending Theory displacement v (mm)	Bending Theory Stress σ_x (N/mm^2)
0	18.28	-743.23	18.37	-843.75
80	18.31	-445.94	18.37	-506.25
160	18.33	-148.65	18.37	-168.75
240	18.34	147.45	18.37	168.75
320	18.36	443.64	18.37	506.25
400	18.37	740.76	18.37	843.75

Table 10: A_3 mix material deflection and bending theory calculation

Depth (mm)	MIF displacement v(mm)	MIF Stress σ_x (N/mm^2)	Bending Theory displacement v(mm)	Bending Theory Stress σ_x (N/mm^2)
0	18.24	-727.56	18.54	-843.75
80	18.28	-436.54	18.54	-506.25
160	18.34	-145.51	18.54	-168.75
240	18.39	145.50	18.54	168.75
320	18.47	437.87	18.54	506.25
400	18.54	723.93	18.54	843.75

Table 11: A_4 mix material deflection and bending theory calculation

Depth (mm)	MIF displacement v(mm)	MIF Stress σ_x (N/mm^2)	Bending Theory displacement v(mm)	Bending Theory Stress σ_x (N/mm^2)
0	19.18	-710.46	19.27	-843.75
80	19.21	-426.28	19.27	-506.25
160	19.24	-142.09	19.27	-168.75
240	19.27	143.18	19.27	168.75
320	19.3	427.67	19.27	506.25
400	19.34	707.43	19.27	843.75

Table 12: A_5 mix material Deflection and bending theory calculation

Depth (mm)	MIF displacement v (mm)	MIF Stress σ_x (N/mm^2)	Bending Theory v (mm)	Bending Theory Stress σ_x (N/mm^2)
0	19.78	-694.54	19.92	-843.75
80	19.81	-416.72	19.92	-506.25
160	19.84	-138.91	19.92	-168.75
240	19.87	139.67	19.92	168.75
320	19.9	417.80	19.92	506.25
400	19.92	691.67	19.92	843.75

The analytical results for displacement and stress (bending), which were determined using MIF and bending theory, are shown in tables from 8 to 12. The graphs for each percentage of replacement along with the depth of the beam are explained below in addition with these findings.

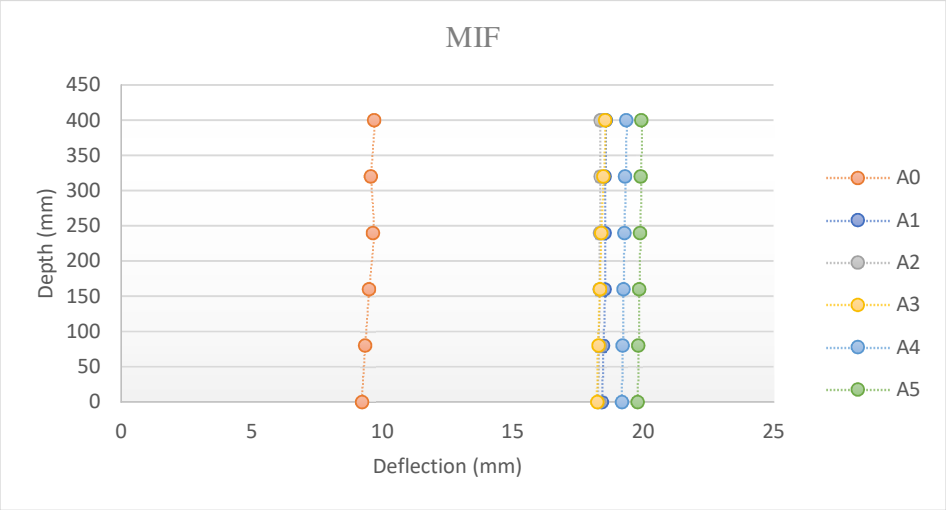

Figure 8: Deflection vs. depth of beam by MIF

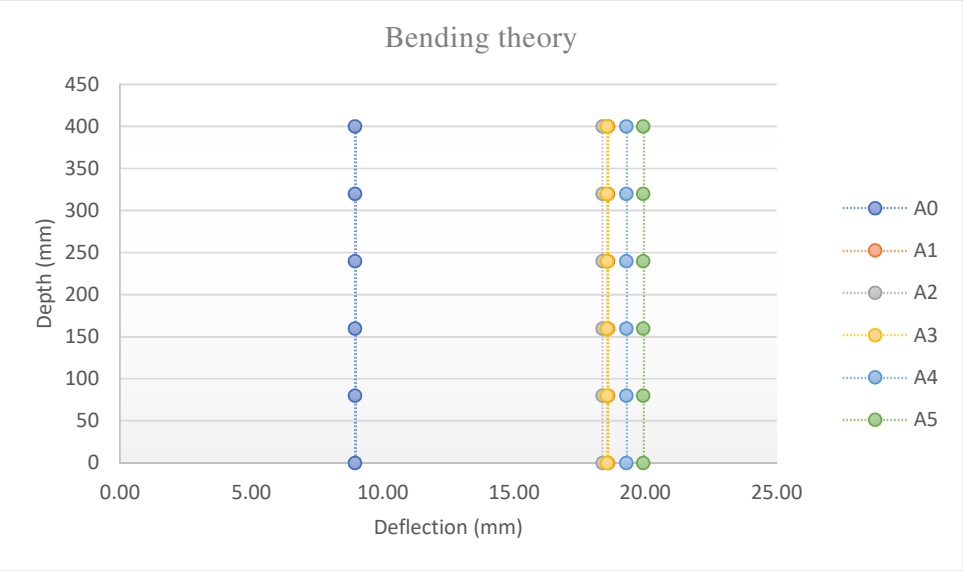

Figure 9: Deflection Vs depth of beam by Bending theory

The displacement variation across the beam's depth is depicted in Figure 8&9. Across the depth, the displacement variation (v) is essentially linear. Displacement depends upon the value of modulus of elasticity of that material **[22].** When compared to the results of the bending theory in Figure 9, the displacement results from MIF reveal in Figure 8 the exact displacement, that is, displacement at different depths of the beam has been illustrated below.

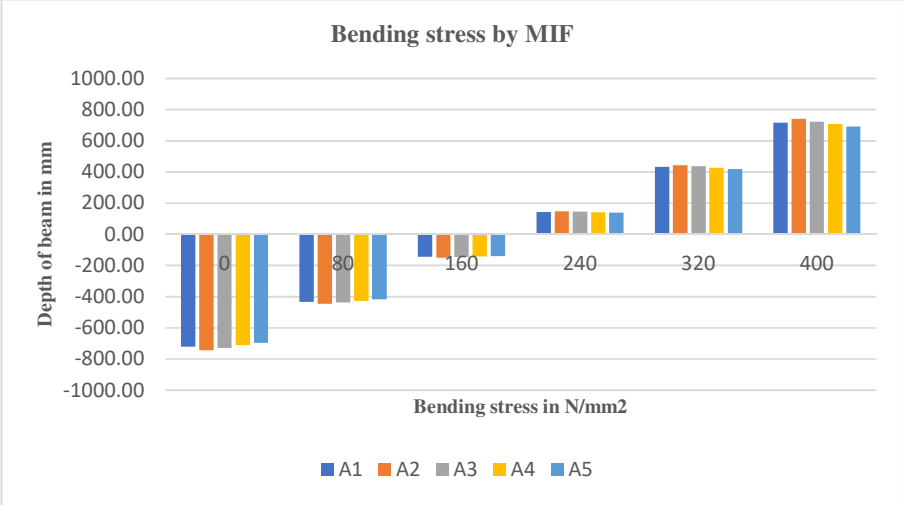

Figure 10(a): Bending stress vs beam depth as calculated using MIF.

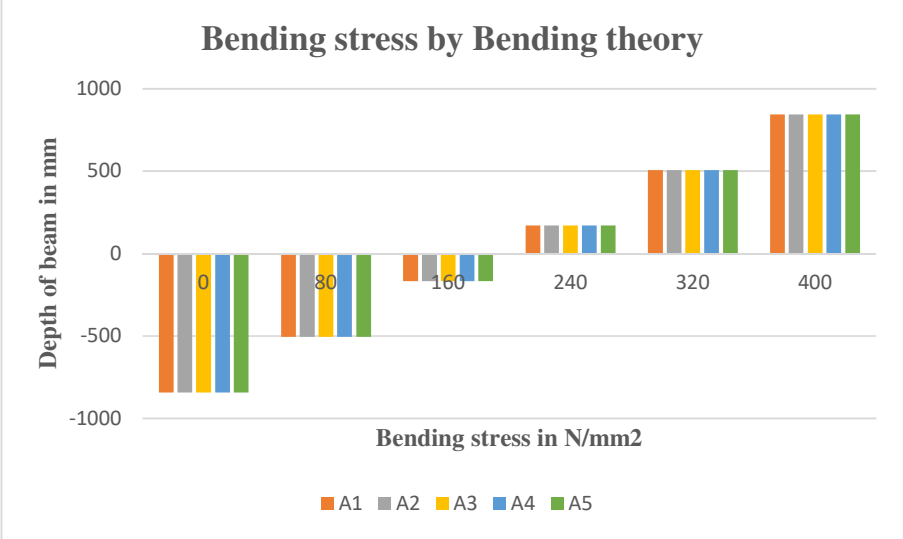

Figure 10(b): Using bending theory calculated a relation between bending stress vs. beam depth.

For various sizes of aggregate replacement, the variation in bending stress over the depth of the beam is shown in Figures 10(a) and (b). Deflection is dependent on the material's elastic modulus value [22]. The graph demonstrates that the MIF and Bending theory stress results are nearly identical. According to the MIF findings, the bending stress has a non-zero value. The bending stress should be zero at the neutral axis and maximum at the top fibres, according to bending theory. By substituting different percentages of coarse aggregates with various sizes of fly ash aggregates in geopolymer concrete, the bending stress lowers as density increases.

6.7. MIF and bending theory comparison: -Figures 11 and 12 show results for the A_2 Combination of fly ash aggregate with normal aggregates in geopolymer concrete. From below figure shows that the displacement of MIF is near the bending theory displacement. While the shape of the line in the case of MIF is irregular, the graph of displacement produced by the bending theory is straight. The displacement results provided by MIF demonstrate an identical or similar displacement, indicating that the displacement at each depth of the beam varies from the results of the bending theory. Slight variation is seen in the beam's displacement of 0.49% at 0 mm depth and 0% variation in beam's displacement at 400 mm depth. (From bottom to top of the beam).

Table 13: Comparison of displacement

Depth (mm)	Deflection (mm)		
	MIF	Bending Theory	% Change
0	18.28	18.37	-0.49
80	18.31	18.37	-0.33
160	18.33	18.37	-0.22
240	18.34	18.37	-0.17
320	18.36	18.37	-0.06
400	18.37	18.37	0.00

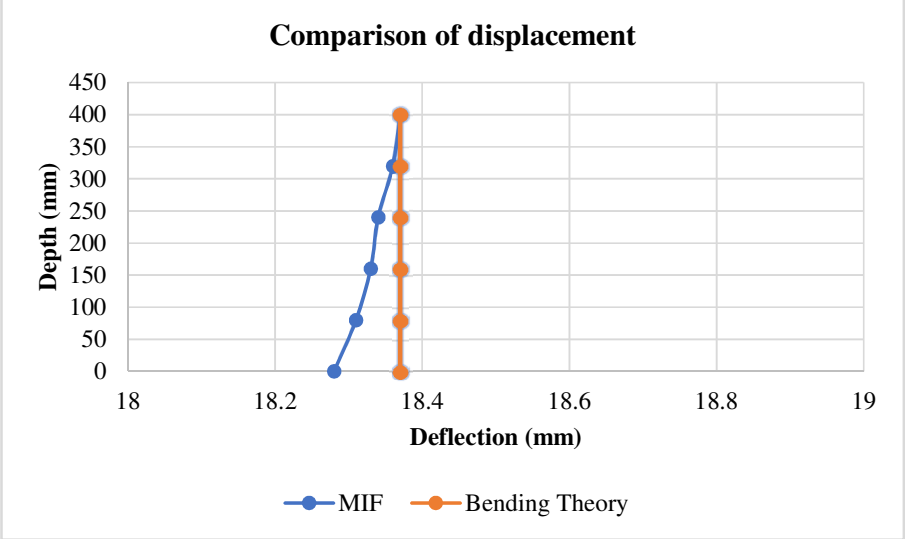

Figure 11: Comparison of displacement by MIF and bending theory

In the case of MIF displacement varies along the depth of the beam and in case of bending theory it is uniform throughout the depth.

Table 14: Comparison of bending stress.

Depth (mm)	Stress σ_x (N/mm^2)		
	MIF	Bending Theory	% Change
0	-743.23	-843.75	-11.91
80	-445.94	-506.25	-11.91
160	-148.65	-168.75	-11.91
240	147.45	168.75	-12.62
320	443.64	506.25	-12.37
400	740.76	843.75	-12.21

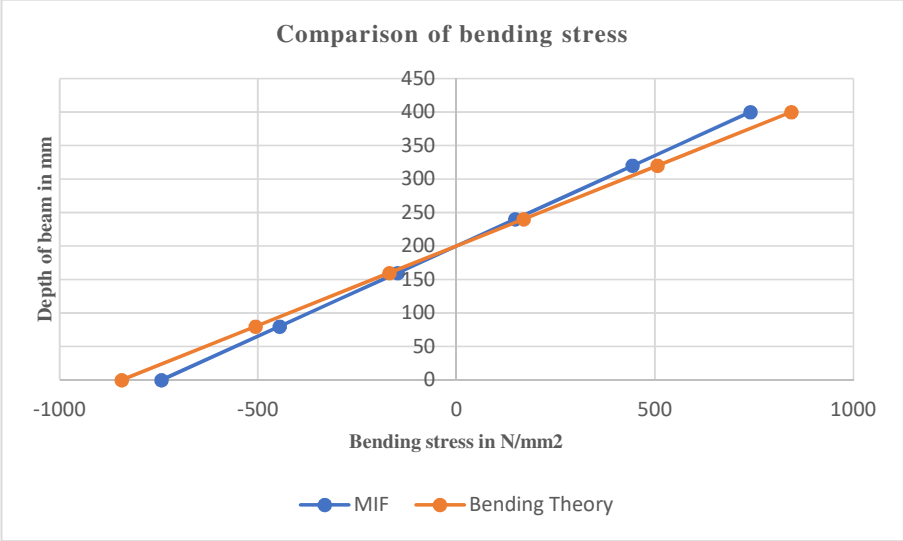

Figure 12: Comparison of bending stress.

From above the figure shows that the bending stress of MIF is nearly the same as the bending stress of the bending theory. The precise variations in stresses and displacements along the depth of the beam are calculated analytically by MIF while considering the elastic material properties. While the assumptions and section characteristics governs bending theory. The Stress deflection results by the Method of Initial Function show the exact results compared to the bending theory findings, as the beam's depth varies. Slight variation is seen in the beam's displacement at -11.91% and -12.21%. (From bottom to top of the beam).

7. Conclusions

Based on the above results, the following conclusions are drawn: -

1. We can Conserve natural coarse aggregates by effective utilization of Sintagg sintered fly ash aggregate in geopolymer concrete.

2. The Sintagg sintered fly ash aggregate has been incorporated in geopolymer concrete without compromising the mechanical strength.
3. This study provides sufficient evidence that we may replace conventional concrete mix with geopolymer concrete in the design of structural components.
4. The MIF model discussed in this study demonstrates the capability to determine stress and displacement outcomes accurately.
5. The MIF method accurately evaluates stress and displacement across the beam's depth, based on the elastic properties of lightweight geopolymer concrete material.
6. The bending theory relies on formulas, whereas the MIF uses the approach of elastic theory.
7. The results from the MIF closely resemble those of the bending theory so MIF is suitable for the analysis of lightweight beams.
8. The results from the MIF were validated by the bending theory, confirming its ability to provide nearly exact values for displacement and stress of lightweight beams (from bottom to top depth).
9. The conclusions highlight the novel use of sintered fly ash aggregates in beams, and the efficiency of the MIF model in analyzing stresses and displacements of lightweight beams.

References

[1] Chen, B. and Liu, J., 2008. Experimental application of mineral admixtures in lightweight concrete with high strength and workability. Construction and Building Materials, 22(6), pp.1108-1113.

[2] Swamy, R.N. and Lixian, W., 1995, June. The ingredients for high performance in structural lightweight aggregate concrete. In Holand et al., editors. Proceedings of the International Symposium on Structural Lightweight Aggregate Concrete 20–24 June 1995, Sandefjord, Norway. Oslo: The Norwegian Concrete Association (pp. 628-639).

[3] Zhang, M.H. and Gjorv, O.E., 1991. Characteristics of lightweight aggregates for high-strength concrete. Materials Journal, 88(2), pp.150-158.

[4] Dolby, P.G., 1995, June. Production and properties of lytag aggregate fully utilized. In Holand et al., editors. Proceedings of the International Symposium on Structural Lightweight Aggregate Concrete 20–24 June 1995, Sandefjord, Norway. Oslo: The Norwegian Concrete Association (pp. 326-335).

[5] Patel, R., Dubey, S.K. and Pathak, K.K., 2020, March. Analysis of Steel Beams for Different Loadings Using MIF. In Indian Structural Steel Conference (pp. 777-786). Singapore: Springer Nature Singapore.

[6] Patel, R., Dubey, S.K. and Pathak, K.K., 2014. Effect of depth span ratio on the behaviour of beams. International Journal of Advanced Structural Engineering (IJASE), 6, pp.1-7.

[7] Patel, R., Dubey, S.K. and Pathak, K.K., 2014. Analysis of isotropic beams using method of initial functions (MIF). Electronic Journal of Structural Engineering, 14, pp.1-6.

[8] Patel, R., Dubey, S.K. and Pathak, K.K., 2014. Application of method of initial functions (MIF) in structural engineering: a review. J. Struct. Eng.(India), 41(3), pp.284-290.

[9] Patel, R., Dubey, S.K. and Pathak, K.K., 2014. Effect of elastic properties on the behaviour of beams. International Journal of Structural Engineering, 5(1), pp.43-53.

[10] Xu, H. and Van Deventer, J.S.J., 2000. The polymerization of alumino-silicate minerals. International journal of mineral processing, 59(3), pp.247-266.

[11] Xu, H. and Van Deventer, J.S., 2000. Ab initio calculations on the five-membered alumino-silicate framework rings model: implications for dissolution in alkaline solutions. Computers & Chemistry, 24(3-4), pp.391-404.

[12] Palomo, A., Grutzeck, M.W. and Blanco, M.T., 1999. Alkali-activated fly ash es: A cement for the future. Cement and concrete research, 29(8), pp.1323-1329.

[13] Hermann, E., Kunze, C., Gatzweiler, R., Kiebig, G. and Davidovits, J., 1999, June. Solidification of various radioactive residues by geopolymer with special emphasis on llong-term stability. In Proceedings of the Geopolymers Conference, Saint-Quentin, France (Vol. 30).

[14] Iyengar, KTS, Chandrashekhara K and Sebastian V.K., 1974.Thick Rectangular Beams, Journal of the Engineering Mechanics Division, Vol.100 (6), p.1277-1282.

[15] Iyengar, K., Raja, T. S, and Raman, P. V., 1979. Free vibration of rectangular beams of arbitrary depth, Acta Mechanica, Vol.32 (1), p. 249-259.

[16] Dubey S.K., 2000. , "analysis of composite laminated deep beam." Proceedings of the third International Conference on Advances in Composites, Bangalore, pp.30-39.

[17] Dubey, S.K., 2005. Analysis of homogeneous orthotropic deep beams, Journal of Structural Engineering, Vol. 32(2), p.109-166.

[18] Patel, R., Dubey, S.K. and Pathak, K.K., 2014. Analysis of infilled beams using method of initial functions and comparison with FEM. Engineering Science and Technology, an International Journal, 17(3), pp.158-164.

[19] Mohammed, A.A., Ahmed, H.U. and Mosavi, A., 2021. Survey of mechanical properties of geopolymer concrete: a comprehensive review and data analysis. *Materials*, *14*(16), p.4690.

[20] Jamal, A.S. Preparation and Properties of Structural Lightweight Aggregate Geopolymer Concrete. Master's Thesis, University of Salahaddin-Erbil, Erbil, Iraq, 2019. Unpublished.

[21] Posi, P.; Teerachanwit, C.; Tanutong, C.; Limkamoltip, S.; Lertnimoolchai, S.; Sata, V.; Chindaprasirt, P. Lightweight geopolymer concrete containing aggregate from recycle lightweight block. Mater. Des. 2013, 52, 580–586.

[22] Cui, Y.; Gao, K.; Zhang, P. Experimental and Statistical Study on Mechanical Characteristics of Geopolymer Concrete. Materials 2020, 13, 1651. [PubMed]

[23] ACI 318 Committee. Building Code Requirements for Structural Concrete; American Concrete Institute: Farmington Hills, MI, USA, 2014.

[24] Nath, P.; Sarker, P.K. Flexural strength and elastic modulus of ambient-cured blended low-calcium fly ash geopolymer concrete. Constr. Build. Mater. 2017, 130, 21–31.

[25] Hassan, A.; Arif, M.; Shariq, M. Effect of curing condition on the mechanical properties of fly ash -based geopolymer concrete. SN Appl. Sci. 2019, 1, 1694.

[26] Shri, M., Kumar, S., Chakrabarty, D., Trivedi, P.K., Mallick, S., Misra, P., Shukla, D., Mishra, S., Srivastava, S., Tripathi, R.D. and Tuli, R., 2009. Effect of arsenic on growth, oxidative stress, and antioxidant system in rice seedlings. Ecotoxicology and environmental safety, 72(4), pp.1102-1110.

[27] Chakrabarti, A.K., Pawar, S.D., Cherian, S.S., Koratkar, S.S., Jadhav, S.M., Pal, B., Raut, S., Thite, V., Kode, S.S., Keng, S.S. and Payyapilly, B.J., 2009. Characterization of the influenza A H5N1 viruses of the 2008-09 outbreaks in India reveals a third introduction and possible endemicity. PloS one, 4(11), p.e7846.

[28] Huang, X., Ranade, R., Ni, W. and Li, V.C., 2013. On the use of recycled tire rubber to develop low E-modulus ECC for durable concrete repairs. Construction and Building Materials, 46, pp.134-141.

[29] Kotresh, K.M. and Belachew, M.G., 2014. Study on waste tyre rubber as concrete aggregates. International Journal of Scientific Engineering and Technology, 3(4), pp.433-436.

[30] Gilbert, I., 2001. Shrinkage, cracking and deflection-the serviceability of concrete structures. Electronic Journal of Structural Engineering, 1(1), pp.15-37.

[31] Asutkar, P., Shinde, S.B. and Patel, R., 2017. Study on the behaviour of rubber aggregates concrete beams using analytical approach. Engineering Science and Technology, an International Journal, 20(1), pp.151-159.